Ferrous Ferric Chloride Downregulates the Inflammatory Response to *Rhodococcus aurantiacus* Infection in Mice

Yimin,*[,a] Huirong Tao,[b] Masashi Kohanawa,[a] Songji Zhao,[c] Yuji Kuge,[d] and Nagara Tamaki[e]

[a] *Department of Advanced Medicine, Graduate School of Medicine, Hokkaido University;* [c] *Department of Tracer Kinetics & Bioanalysis, Graduate School of Medicine, Hokkaido University;* [d] *Central Institute of Isotope Science, Hokkaido University;* [e] *Department of Nuclear Medicine, Graduate School of Medicine, Hokkaido University; Kita 15, Nishi 7, Kita-ku, Sapporo, 060–8638, Japan: and* [b] *Tao Clinic; Kita 21, Nishi 5, Kita-ku, Sapporo 001–0021, Japan.*
Received July 30, 2012; accepted September 1, 2012; advance publication released online September 24, 2012

The healthy drink Pairogen is mainly composed of ferrous ferric chloride water that reportedly changes the status of intracellular water from oxidative to antioxidative. Here, we investigated whether Pairogen affects host immune function in a murine model of granulomatous inflammation in response to *Rhodococcus aurantiacus* (*R. aurantiacus*) infection. Longitudinal ingestion of Pairogen markedly improved the survival of infected mice in a concentration-dependent manner. Compared to mice received water, mice that ingested 10-fold-diluted Pairogen displayed rapid bacterial elimination, decreased production of tumor necrosis factor (TNF)-α and interleukin (IL)-6, and high levels of IL-10 in organs during the initial phase of infection. Moreover, histological studies showed significant reduction in the number and size of granulomas as well as amelioration of oxidative stress in the livers of mice ingested 10-fold-diluted Pairogen at 14 d post-infection. These characteristics were further pronounced in first-generation (F1) mice that also ingested 10-fold-diluted Pairogen. Following stimulation with heat-killed *R. aurantiacus*, the production of TNF-α, IL-6, and IL-10 by macrophages from F1 mice was similar to that detected *in vivo*, while their gene expression levels in these cells were significantly lower than the levels in macrophages from mice received water. Heat-killed *R. aurantiacus* also induced the expression of heme oxygenase-1 mRNA in the cells from F1 mice. Taken together, these results indicate that Pairogen contributes to the negative regulation of the immuno-inflammatory response to *R. aurantiacus* infection in mice by modulating the cellular redox state. Longitudinal ingestion of Pairogen further enhances the defense function in mouse progeny.

Key words Pairogen; ferrous ferric chloride; immuno-inflammatory response; *Rhodococcus aurantiacus*; redox state; mouse

The healthy drink Pairogen (Akatsuka Co., Mie, Japan) consists of 90% ferrous ferric chloride (FFC) water and 10% purified ingredients, including rice vinegar, Japanese apricot vinegar, apple vinegar, persimmon vinegar, vitamin B_2, vitamin B_6, vitamin C, glucose, fructose, citric acid, and malic acid.[1,2] FFC is a special aqueous iron composed of a complex of ferrous chloride and ferric chloride and is known to participate in intracellular redox reactions.[3,4] FFC water is obtained by immersing FFC ceramic beads (Akatsuka Co.) in water. Pairogen and FFC water are reported to influence multiple biological functions in living organisms. For example, Hasegawa *et al.* demonstrated that FFC water stimulates plant growth, particularly that of roots.[5] The addition of either FFC water or Pairogen to a medium showed an equal effect on inducing the proliferation and differentiation of epidermal cells derived from both humans and mice.[1,4,6] Moreover, treating mice with skin lotion containing FFC stimulates the proliferation and differentiation of skin cells as well as hair growth.[7] However, little is known about the effects of FFC and Pairogen on modulating immune defense functions in animals or humans.

In response to microbial pathogen invasion, the host immune system is quickly activated *via* pattern-recognition receptors, leading to the innate immune response in which the release of various inflammatory mediators and the recruitment of inflammatory cells constitute the host's primary line of defense during the initial stages of infection.[8,9] Pro-inflammatory cytokines such as tumor necrosis factor (TNF)-α and interleukin (IL)-1β, as critical inflammatory mediators, initiate an inflammatory cascade to eliminate pathogens and promote tissue repair, whereas the generation of anti-inflammatory cytokines is essential for limiting an uncontrolled hyperinflammatory response.[10,11] The balance between pro-inflammatory and anti-inflammatory cytokines in the innate immune response not only plays key roles in homeostasis maintenance and host survival, but also influences the severity and duration of the adaptive immune response.[12,13] Increasing evidence indicates that several inflammation-related processes, including regulation of pro-inflammatory and anti-inflammatory cytokine production, depend on cellular redox signaling. Augmented oxidative stress such as overproduction of reactive oxygen species results in increased gene expression and secretion of pro-inflammatory cytokines and initiates tissue damage.[14–16] In contrast, an antioxidant response involving generation of antioxidant enzymes and the addition of antioxidant agents negatively regulates the inflammatory response.[17,18] Therefore, maintenance of redox homeostasis is critical for host immune function. *Rhodococcus aurantiacus* (*R. aurantiacus*) is an intracellular psychrophilic Gram-positive bacterium closely related to members of the genera *Corynebacterium*, *Mycobacterium*, and *Nocardia*. Infection with *R. aurantiacus* induces a non-necrotic and epithelioid granulomatous inflammation in mice, which resembles human sarcoidosis.[19] Our previous studies have demonstrated that this inflammatory response is mainly regulated by the balance between TNF-α, IL-6, and IL-10 production during the initial phase of infection.[20]

In the present study, we assessed the role of Pairogen in regulating the immuno-inflammatory response to *R. aurantiacus* infection in mice. Our results indicate that longitudinal

The authors declare no conflict of interest.

* To whom correspondence should be addressed. e-mail: yimin@med.hokudai.ac.jp

ingestion of Pairogen suppressed an excessive inflammatory response in mice and that the immune defense function was further enhanced in their progeny when they were also treated with Pairogen.

MATERIALS AND METHODS

Mice Pairogen was supplied by Akatsuka Co. and diluted 1000-, 100-, and 10-fold with sterile water. Female and male C57BL/6 mice purchased from SLC Inc. (Shizuoka, Japan) were used as the parental generation (P mice). The animal protocol was approved by the Institutional Animal Care and Use Committee of Hokkaido University. After 7 d of acclimatization, 4-week-old female P mice received 1000-, 100-, or 10-fold-diluted Pairogen, and male P mice were given a drink of 10-fold-diluted Pairogen. Breeding of male and female P mice received 10-fold-diluted Pairogen produced the first generation of progeny (F1 mice), which also received 10-fold-diluted Pairogen after weaning. Eight-week-old female P and F1 mice were used for *in vivo* infection studies, and male F1 mice were used for *in vitro* experiments. P and F1 mice that received sterile water were used as controls. All the mice were housed in a temperature-controlled room with a 12-h light/dark diurnal cycle and had free access to food and drink throughout the experiment.

Infection of Mice with *R. aurantiacus* Female P and F1 mice that received 1000-, 100-, 10-fold-diluted Pairogen or sterile water, were inoculated *via* a lateral tail vein with 1×10^8 colony forming units (CFU) of viable *R. aurantiacus* (strain 80005) suspended in 0.2 mL of phosphate-buffered saline (PBS). 0.2 mL of PBS was injected as a control for *R. aurantiacus*. The survival of the mice was monitored daily up to 14 d post-infection, and survival curves were plotted.

Determination of the Bacterial Counts in Organs Tissues were harvested from infected mice at the indicated times post-infection and homogenized in RPMI 1640 medium (Sigma, MO, U.S.A.) (0.1 g/10 mL); 100 μL of the organ homogenates and their serial 10-fold dilutions were plated onto nutrient agar plates (Nissui Pharmaceutical Co., Ltd., Tokyo, Japan). Viable colonies were counted at 48 h after culture. Using this method, we could detect $>10^3$ bacteria/g of organ.

Preparation of Organ Extracts The murine spleens and livers were aseptically removed at the indicated times post-infection and suspended in RPMI 1640 medium containing 1% (w/v) CHAPS (Wako Pure Chemical Industries, Ltd., Kyoto, Japan). Ten percent (w/v) homogenates were prepared with a Dounce grinder. The homogenates were clarified by centrifugation at 2000×***g*** for 30 min, and the supernatants were stored at −80°C for cytokine assays.

Peritoneal Macrophages Culture The peritoneal macrophages were harvested from uninfected 8-week-old F1 male mice treated with 10-fold-diluted Pairogen or sterile water and suspended in 0.83% ammonium chloride solution containing 10% (v/v) Tris buffer (pH 7.65) to lyse erythrocytes. The cells were resuspended in RPMI 1640 medium supplemented with 10% fetal bovine serum (FBS), 100 IU/mL penicillin, and 100 mg/mL streptomycin, and then dispensed into 24-well plates at 5×10^5 cells/well for cytokine assays and 35-mm dishes at 2×10^6 cells/dish for RNA extraction. After culture for 2 h at 37°C, floating cells were removed, and the attached macrophages were further cultured for 12 h and then stimulated with heat-killed *R. aurantiacus* (multiplicity of infection (MOI) of 2).

Measurement of Cytokine Production Enzyme-linked immunosorbent assay (ELISA) was used to determine cytokine concentrations in the organ extracts and culture supernatants. The TNF-α level was determined as described previously.[21] A purified hamster anti-TNF-α monoclonal antibody (mAb) and a purified rabbit anti-TNF-α polyclonal antibody (Endogen, MA, U.S.A.) were used as capture and detection antibodies, respectively. A standard curve was constructed for each experiment by serially diluting recombinant TNF-α (R&D systems, Minneapolis, MN, U.S.A.). IL-6 concentration was also measured by ELISA. Plates were coated with purified rat anti-IL-6 mAb (BD Bioscience, Inc., CA, U.S.A.) and incubated with culture supernatants or organ extracts. IL-6 was detected with a biotinylated rat anti-IL-6 mAb (BD Bioscience, Inc.). All ELISAs were run with recombinant IL-6 (BD Bioscience, Inc.). IL-10 concentrations were measured using the DuoSet ELISA development kit (R&D systems) according to the manufacturer's protocol. The sensitivities of the ELISAs were 50 pg/mL for TNF-α and 20 pg/mL for IL-6 and IL-10.

Quantitative Real-Time Polymerase Chain Reaction (PCR) analysis Total RNA was isolated from peritoneal macrophages using the Trizol reagent (Invitrogen, CA, U.S.A.) and reverse transcribed to first-strand cDNA using the Moloney murine leukemia virus reverse transcriptase (TOYOBO Co., Osaka, Japan). The cDNA was utilized for quantitative real-time PCR with the Power 2× SYBR Green PCR master mix and monitored on an ABI Prism 7000 sequence detection system (both from Applied Biosystems, CA, U.S.A.). The PCR conditions were 95°C for 10 min followed by 40 cycles at 95°C for 15 s and 60°C for 1 min. The primer sequences of the

Table 1. Primers Used for Quantitative Real-Time PCR

Gene name	Direction	Primer sequence	Amplicon size (bp)	Accession No.
TNF-α	Forward	5′-GGGTGATCGGTCCCCAAAGG-3′	95	NM_013693
	Reverse	5′-TTGAGAAGATGATCTGAGTGTGAGG-3′		
IL-6	Forward	5′-AAGAAATGATGGATGCTACCAAACTG-3′	79	NM_031168
	Reverse	5′-GTACTCCAGAAGACCAGAGGAAATT-3′		
IL-10	Forward	5′-GGACAACATACTGCTAACCGACTC-3′	73	NM_010548
	Reverse	5′-TTCCGATAAGGCTTGGCAACC-3′		
NF-κB	Forward	5′-CCACTGTCTGCCTCTCTCGTC-3′	97	NM_008689
	Reverse	5′-GAAGGATGTCTCCACACCACTG-3′		
HO-1	Forward	5′-TTCCTGCTCAACATTGAGCTGTT-3′	86	NM_010442
	Reverse	5′-GACGCCATCTGTGAGGGACT-3′		

selected genes are shown in Table 1. Relative gene expression *vs.* untreated control was normalized by using the expression of the glyceraldehyde-3-phosphate dehydrogenase (GAPDH) housekeeping gene.

Histological Analysis Animals were sacrificed, and the removed liver samples were fixed in 10% neutral formalin and embedded in paraffin blocks. Tissue sections of 2 μm were stained with hematoxylin and eosin (H&E) using standard techniques. In each experiment, sections were made from three different areas of each organ. The size of the granuloma was calculated by the diameter of each granuloma measured with an ocular micrometer. The mean size of a granuloma and the mean number of granulomas per field were measured from four random optical fields within each section. Granuloma area was determined from the size of granuloma multiplied by the number of granulomas. Paraffin sections were also used for immunohistochemistry of 8-hydroxy-2′-deoxyguanosine (8-OHdG), a marker of oxidative DNA damage. The sections were stained with mouse anti-mouse 8-OHdG (Japan Institute for the Control of Aging, Shizuoka, Japan), followed by application of the immunoperoxidase technique using the STAT-Q rapid IHC system (Innovex Biosciences, CA, U.S.A.). As a negative control, slides were incubated with normal mouse immunoglobulin G (IgG) (Santa Cruz Biotechnology Inc., CA, U.S.A.). Stained cells were quantified using the Image J software, and the data are expressed as the number of cells per field.

Statistical Analysis All the data are expressed as mean± standard deviation (S.D.). Significant differences between the values in the mouse groups were calculated using Student's *t* tests or one-way analysis of variance (ANOVA) with Tukey's *post-hoc* tests. The *p*-values of <0.05 were considered statistically significant.

RESULTS

Effect of Pairogen on the Survival of Infected Mice Mice in each group were inoculated with 1×10^8 CFU of viable *R. aurantiacus*, and survival was monitored for 14 d. The P and F1 mice that received water showed a 70% survival rate at 14 d post-infection (Fig. 1A). Although no significant difference was observed in the survival rate for the P mice received water and those treated with either 1000- or 100-fold-diluted Pairogen, P mice treated with 10-fold-diluted Pairogen had an 85% survival rate at 14 d post-infection (Fig. 1A). Higher survival rates were also observed in the F1 mice treated with 1000- or 100-fold-diluted Pairogen relative to those received water (80, 90%, respectively); moreover, all the F1 mice treated with 10-fold-diluted Pairogen survived over 14 d after infection (Fig. 1B). PBS injection had no effect on the survival of mice receiving either Pairogen or water (data not shown).

Effect of Pairogen on Bacterial Elimination in Infected Mice After challenge with *R. aurantiacus*, the *in vivo* kinetics of bacterial growth and elimination in P and F1 mice treated with 10-fold-diluted Pairogen were compared with those in P and F1 mice received water. Bacterial proliferation was undetectable in each group of infected mice (Fig. 2). The P and F1 mice that received water displayed a decrease in bacterial burden in their livers and spleens, which fell to an undetectable level at 11 d post-infection (Fig. 2). In contrast, the bacterial counts rapidly declined and were no longer

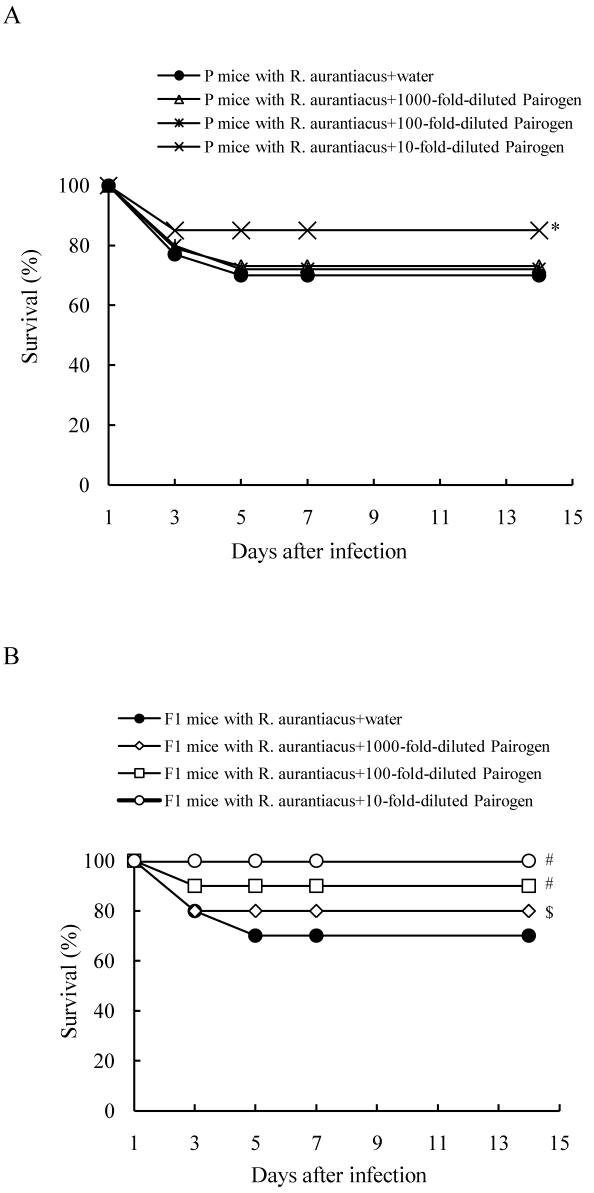

Fig. 1. Survival Rates of Mice

After infection with 1×10^8 CFU of *R. aurantiacus*, the survival rates of P mice treated with water or 1000-, 100-, 10-fold-diluted Pairogen from 4 weeks of age (A); and F1 mice that were also treated with water or 1000-, 100-, 10-fold-diluted Pairogen after weaning (B) were determined over a 14-d experimental period. Each data point was generated from 2 independent experiments in which 10 mice per group were used. $^{\$}p<0.05$, $^{*}p<0.01$, $^{\#}p<0.001$ *vs.* P or F1 mice treated with water.

detectable at 9 d post-infection in the organs of P mice treated with 10-fold-diluted Pairogen, and at 7 d post-infection in the spleens and at 8 d post-infection in the livers of F1 mice treated with 10-fold-diluted Pairogen (Fig. 2).

Effect of Pairogen on Cytokine Production in Infected Mice Because the balance between pro-inflammatory and anti-inflammatory cytokine production in the early phase of *R. aurantiacus* infection plays key roles in mouse survival and the development of granulomatous inflammation,[20,21] we investigated the effect of Pairogen on cytokine secretion. There was no cytokine secretion detected in the organs of P and F1 mice that ingested Pairogen alone (Figs. 3A–C). Infection with *R. aurantiacus* induced a high level of TNF-α in the spleens of P and F1 mice that received water on days 1–7

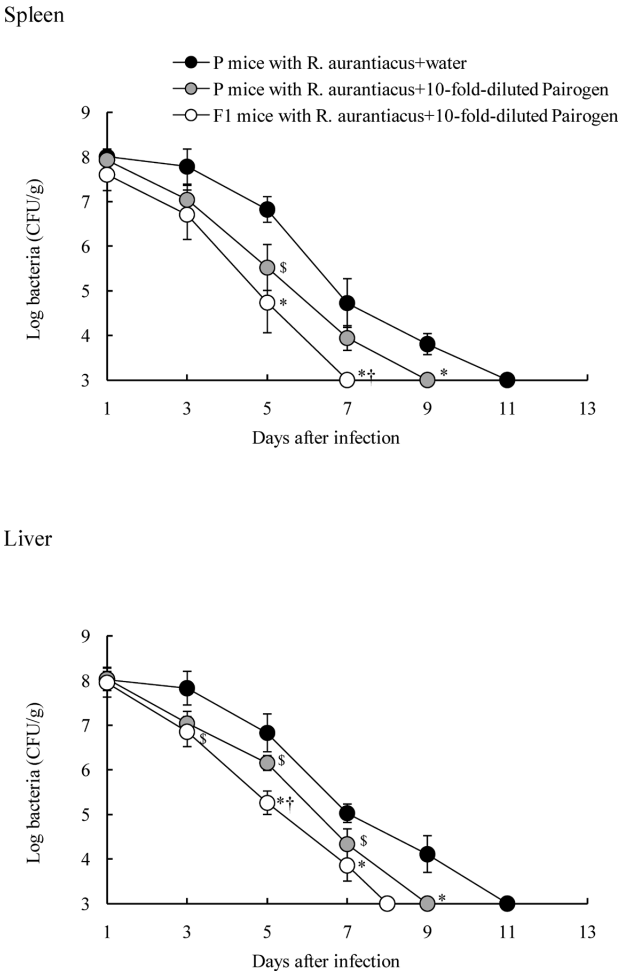

Fig. 2. Kinetics of Bacterial Load in Mouse Organs

After infection with 1×10^8 CFU of *R. aurantiacus*, the numbers of viable bacteria present in the spleens and livers of P and F1 mice treated with water or 10-fold-diluted Pairogen were determined over a 14-d experimental period. The results are represented by mean±S.D. values from 2 independent experiments in which 3 mice per group were used at each time point. $^{\$}p<0.05$, $^{*}p<0.01$ *vs.* P mice treated with water; $^{\dagger}p<0.05$ *vs.* P mice treated with 10-fold-diluted Pairogen.

post-infection and in their livers on days 1–5 post-infection; in contrast, P and F1 mice treated with 10-fold-diluted Pairogen showed a significant decrease in TNF-α production in organs in the early phase of infection, especially F1 mice (Fig. 3A). The mice received water also exhibited peak levels of IL-6 in spleens at 3 d post-infection and in livers at 1 d post-infection; thereafter, IL-6 production gradually diminished through 7 d (Fig. 3B). A marked reduction in IL-6 release was noted on days 1–7 post-infection in the organs of P mice treated with 10-fold-diluted Pairogen, and this reduction was even more pronounced in F1 mice treated with 10-fold-diluted Pairogen (Fig. 3B). The IL-10 level was also measured in the organ extracts from infected mice. A peak splenic value of IL-10 was observed at 1 d post-infection in P and F1 mice received water, and thereafter gradually decreased until 7 d, while the level of IL-10 was barely detectable in their livers (Fig. 3C). Although there was no significant change in splenic IL-10 production between the two mouse groups, the IL-10 level on days 1–3 post-infection in the livers of P mice treated with 10-fold-diluted Pairogen was higher than that in P mice received water (Fig. 3C). Moreover, F1 mice treated with 10-fold-diluted Pairogen showed a further increase in IL-10 production in spleens on days 3–7 post-infection and in livers on days 1–3 post-infection (Fig. 3C). PBS injection did not induce any cytokine production in the organs of the mice from each group (data not shown).

Effect of Pairogen on Mouse Macrophages Following *R. aurantiacus* Challenge Because TNF-α, IL-6, and IL-10 are produced principally by macrophages in response to bacterial infection,[22,23] we further investigated the secretion and mRNA expression of these cytokines in the peritoneal macrophages from Pairogen-treated mice following stimulation with heat-killed *R. aurantiacus*. TNF-α level in control macrophages that were isolated from F1 mice received water peaked at 24 h post-stimulation, and decreased gradually thereafter (Fig. 4A). Although a peak level of TNF-α was also observed in the macrophages from F1 mice treated with 10-fold-diluted Pairogen at 24 h post-stimulation, its production significantly attenuated from 12 h post-stimulation compared with that in the controls (Fig. 4A). Control macrophages exhibited a lasting increase in IL-6 secretion over a 48-h stimulation period, whereas IL-6 release dramatically declined in the cells from F1 mice treated with 10-fold-diluted Pairogen (Fig. 4A). Stimulation with heat-killed *R. aurantiacus* also resulted in a gradual elevation of IL-10 secretion in control macrophages at least until 48 h, and a further increase in IL-10 level was detected in the culture supernatant of the cells from F1 mice treated with 10-fold-diluted Pairogen (Fig. 4A).

Furthermore, heat-killed *R. aurantiacus* also up-regulated the gene expression levels of TNF-α, IL-6, and IL-10 in control macrophages, which peaked at 3, 12, and 1 h post-stimulation, respectively (Fig. 4B). However, lower levels of TNF-α and IL-6 mRNA expression, particularly of IL-6, were found in the cells from F1 mice treated with 10-fold-diluted Pairogen (Fig. 4B). Interestingly, whereas IL-10 secretion augmented, the level of IL-10 mRNA expression was significantly suppressed in these cells at 1–3 h post-stimulation (Fig. 4B).

We also determined the gene expression of nuclear transcription factor (NF)-κB in mouse macrophages, which is an important transcription factor involved in inflammatory and immune responses. Following stimulation, the level of NF-κB mRNA expression was augmented and peaked at 3 h in control macrophages; however, this elevation was significantly down-regulated at 1–3 h in the cells from F1 mice treated with 10-fold-diluted Pairogen (Fig. 4C). Heme oxygenase-1 (HO-1), which provides a defense mechanism against inflammation, is mainly produced by macrophages.[24] In *in vitro* experiments, exposure to heat-killed *R. aurantiacus* also induced an increase in the level of HO-1 mRNA expression at 6–12 h post-stimulation in the macrophages from F1 mice treated with 10-fold-diluted Pairogen compared with that in the controls (Fig. 4C).

Effect of Pairogen on Granuloma Formation and Redox State in Livers After *R. aurantiacus* was injected, hepatic histological changes were compared between the mice received water and those treated with 10-fold-diluted Pairogen at 14 d, which is a sufficient time for granuloma formation. A large number of non-necrotic and epithelioid granulomas were observed in the livers of P and F1 mice received water (mean area of granulomas per field, 36.8%), and treatment with 10-fold-diluted Pairogen significantly decreased the number and size of granulomas in the livers of P and F1 mice, particularly in the latter (28.7, 18.3%, respectively) (Fig. 5A). The

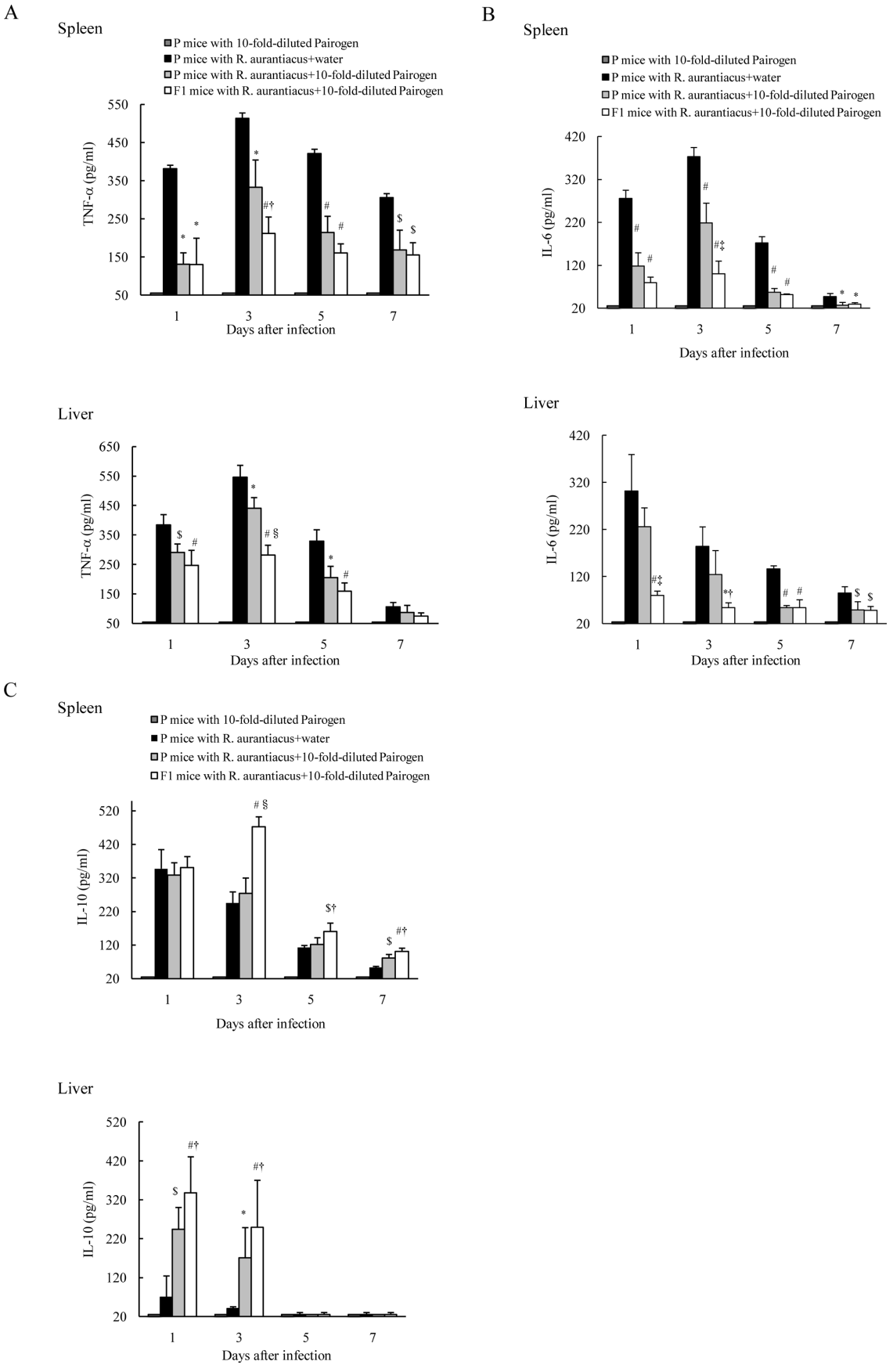

Fig. 3. Kinetics of Cytokine Production in Mouse Organs

After infection with 1×10^8 CFU of *R. aurantiacus* or uninfection, the production of TNF-α (A), IL-6 (B), and IL-10 (C) were measured on days 1–7 in the spleens and livers of P and F1 mice treated with water or 10-fold-diluted Pairogen. The results represent the mean±S.D. values from 2 independent experiments in which 3 mice per group were used at each time point. $^{\$}p<0.05$, $^{*}p<0.01$, $^{\#}p<0.001$ *vs.* P mice treated with *R. aurantiacus* and water; $^{\dagger}p<0.05$, $^{\ddagger}p<0.01$, $^{\S}p<0.001$ *vs.* P mice treated with *R. aurantiacus* and 10-fold-diluted Pairogen.

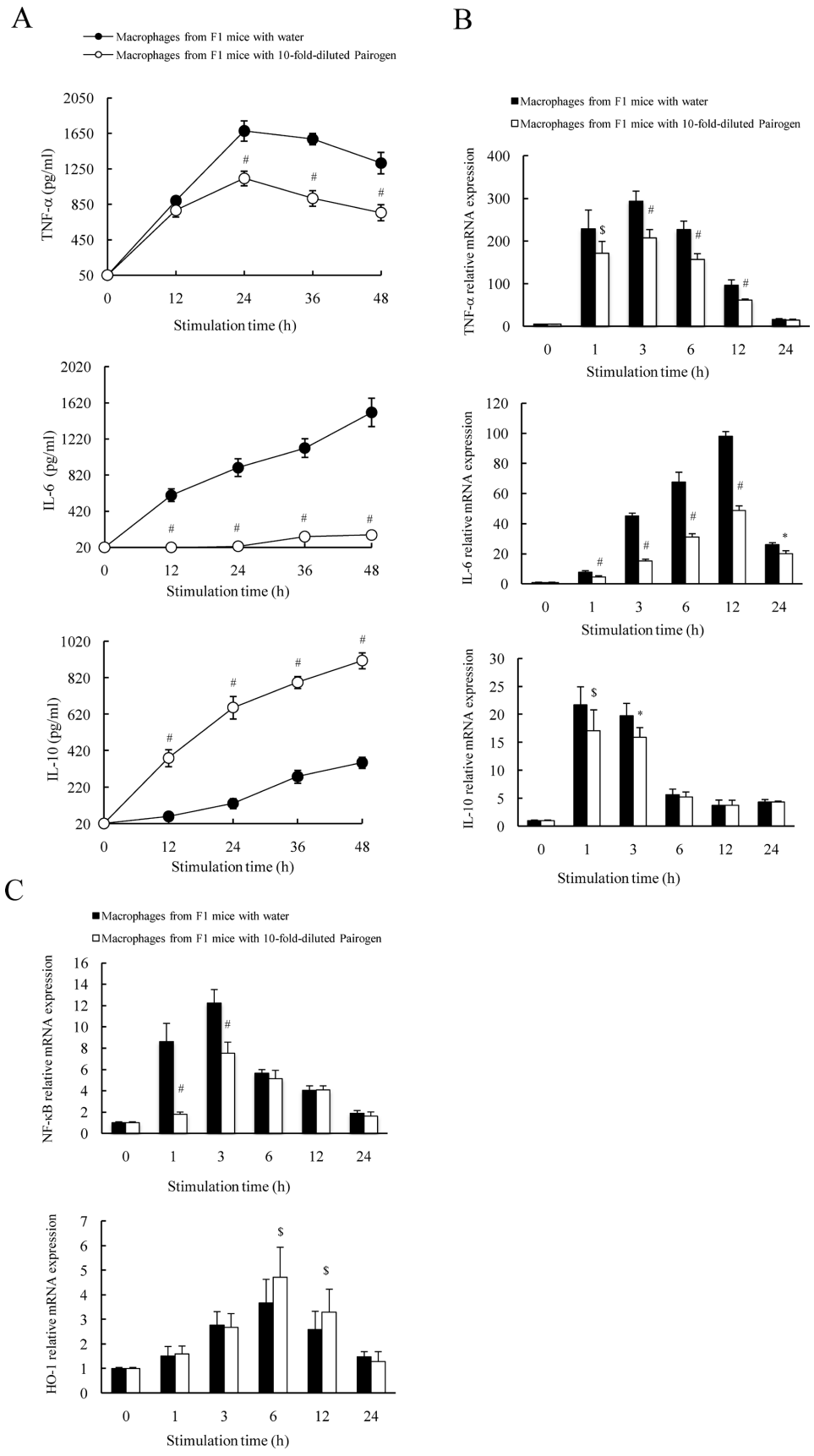

Fig. 4. Expression of Cytokines, NF-κB, and HO-1 by Mouse Macrophages

Under condition of stimulation with heat-killed *R. aurantiacus* (MOI 2), the production of TNF-α, IL-6, and IL-10 (A), and their gene expression (B) as well as the gene expression of NF-κB and HO-1 (C) were measured in the peritoneal macrophages from F1 mice treated with water and those treated with 10-fold-diluted Pairogen. The results represent the mean±S.D. values from 3 independent experiments. $^{\$}p<0.05$, $*p<0.01$, $^{\#}p<0.001$ *vs.* cells from F1 mice treated with water.

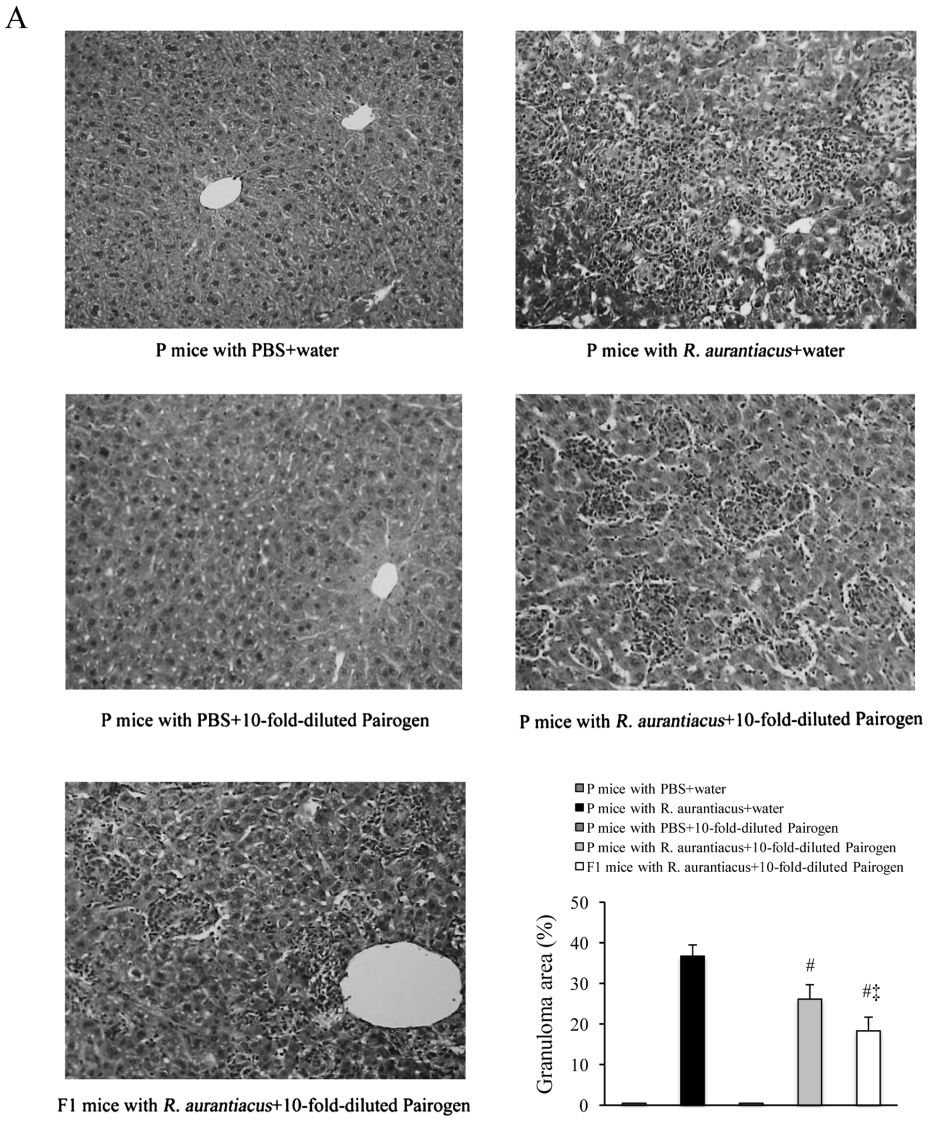

Fig. 5A. Histological Analysis of Mouse Livers at 14 d Post-Infection

(A) Representative H&E-stained liver sections (original magnification, ×200) and the percentage of granuloma areas. The results are expressed as the mean±S.D. values of 5–7 mice per group. $^{\#}p<0.001$ *vs.* P mice treated with *R. aurantiacus* and water; $^{\ddagger}p<0.01$ *vs.* P mice treated with *R. aurantiacus* and 10-fold-diluted Pairogen.

immunohistochemical analysis results for 8-OHdG are shown in Fig. 5B. At 14 d post-infection, a significant population of 8-OHdG-positive cells was observed throughout the lobules of mice received water (73/field). In contrast, there was a marked decrease in the number of these cells in the lobules of P and F1 mice that were treated with 10-fold-diluted Pairogen (59, 40/field, respectively). PBS injection and Pairogen ingestion did not induce detectable histological changes in the livers of mice (Figs. 5A, B).

DISCUSSION

To our knowledge, the present study is the first to indicate that the healthy drink Pairogen contributes to the modulation of host inflammatory and immune responses to bacterial infection. Compared with mice ingested water, P and F1 mice that were longitudinally ingested serial dilutions of Pairogen showed enhanced resistance to *R. aurantiacus* infection. Moreover, all F1 mice treated with 10-fold-diluted Pairogen survived infection. However, administration of 10-fold-diluted Pairogen just before or just after bacterial infection failed to augment mouse resistance and survival (data not shown). FFC water, which is the main component of Pairogen, reportedly regulates cellular functions by changing the state of intracellular water from oxidative to antioxidative.[3,4] It has also been reported that a well-controlled homeostatic redox balance is the most critical event for host survival during host-microbe interaction in *Drosophila*.[25] Considering our observations and these previous reports, we conclude that the improved natural resistance of mice to *R. aurantiacus* resulted from the well-regulated cellular redox state due to long-term ingestion of Pairogen.

It is well known that an imbalanced cytokine response to invading pathogens results in aggravated immune responses, septic shock, and even death.[14,26] Our previous studies have also shown that the excessive production of TNF-α and IL-6 during the initial phase of *R. aurantiacus* infection is responsible for mouse death, although the clearance of bacteria

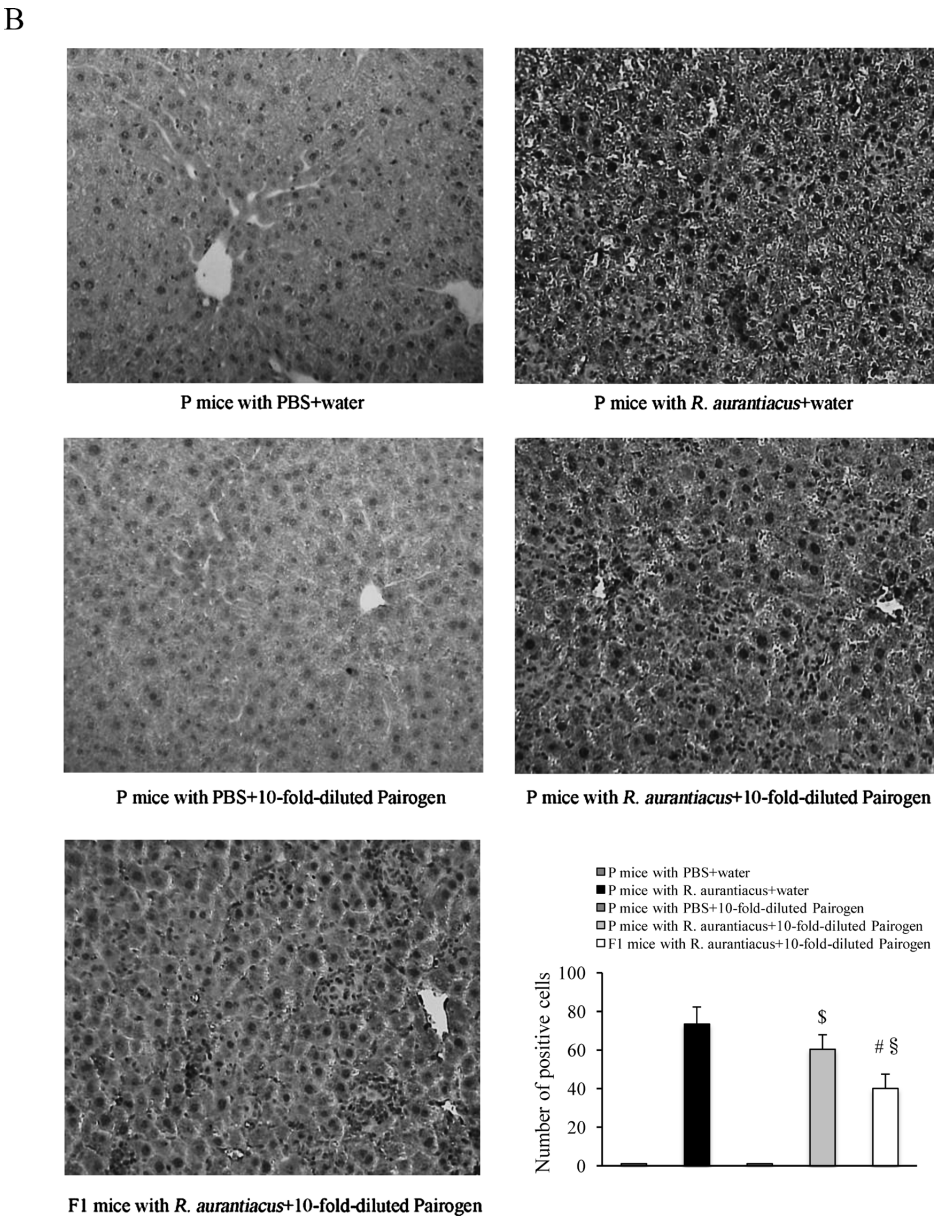

Fig. 5B. Histological Analysis of Mouse Livers at 14 d Post-Infection

(B) Representative images (original magnification, ×200) of immunohistochemistry for 8-OHdG in livers and the number of positively stained cells per field. Nuclei stained brown indicate positive immunoreactivity to a monoclonal antibody against 8-OHdG. The results are expressed as the mean±S.D. values of 5–7 mice per group. $^{\$}p<0.05$, $^{\#}p<0.001$ *vs.* P mice treated with *R. aurantiacus* and water; $^{\S}p<0.001$ *vs.* P mice treated with *R. aurantiacus* and 10-fold-diluted Pairogen.

depends on the presence of TNF-α, but not of IL-6.[21,27] In the present study, after challenge with *R. aurantiacus*, P and F1 mice treated with 10-fold-diluted Pairogen exhibited significant decreases in TNF-α and IL-6 secretion and bacterial burden in organs compared with those received water, particularly the F1 mice. Similarly, macrophages from F1 mice treated with 10-fold-diluted Pairogen expressed reduced levels of TNF-α and IL-6 as well as reduced mRNA expression under stimulatory condition. Therefore, it is evident that longitudinal administration of Pairogen suppressed the excessive expression of TNF-α and IL-6 when mice were infected with *R. aurantiacus*, which subsequently led to acceleration of bacterial clearance and amelioration of survival. NF-κB is a redox-sensitive transcription factor,[16,28] and its expression and activity are inhibited by antioxidants such as *N*-acetylcysteine and butyrate in lipopolysaccharide (LPS)-induced inflammation.[29,30] In the current study, the macrophages from F1 mice treated with 10-fold-diluted Pairogen also showed a decreased level of NF-κB gene expression triggered by heat-killed *R. aurantiacus*. This result suggests that Pairogen contributes to the negative regulation of NF-κB gene expression in macrophages, which results in a decrease in the gene expression levels of TNF-α and IL-6, because the expression of these genes is reported to be regulated by NF-κB.[29,31] In the macrophages from F1 mice treated with 10-fold-diluted Pairogen, the elevation in IL-10 mRNA expression induced by heat-killed *R. aurantiacus* was mildly but significantly attenuated compared with that in the cells from F1 mice received water. Although the molecular mechanism by which IL-10 gene expression is regulated is not well understood, a number of studies have

reported the inhibitory effects of antioxidants on IL-10 expression and secretion.[29,32] Of interest, in contrast to a reduction in the mRNA expression level of IL-10, a continuous augmentation of its secretion was found in the macrophages from F1 mice treated with 10-fold-diluted Pairogen following stimulation. Consistent with the *in vitro* results, P and F1 mice treated with 10-fold-diluted Pairogen also showed a higher level of IL-10 in the initial phase of infection, relative to the mice received water, especially the F1 mice. Our previous studies have demonstrated that TNF-α, IL-6, and IL-10 are negatively regulated by each other in the inflammatory response to *R. aurantiacus* infection and that the balance among the three cytokines determines the development of granulomatous inflammation.[20,21] Hence, we consider the increased release of IL-10 in mice treated with 10-fold-diluted Pairogen and their macrophages to be due to reduction in TNF-α and IL-6 production. Although several antioxidants have been reported to interfere early in inflammatory responses by blocking or modifying the signal transduction of cytokines,[33–35] administration of 10-fold-diluted Pairogen just before or just after *R. aurantiacus* infection did not show any effects on cytokine expression and the development of inflammation in mice (data not shown).

Following *R. aurantiacus* infection, there was significant amelioration of oxidative stress in the livers of P and F1 mice treated with 10-fold-diluted Pairogen compared with that in mice received water, which was accompanied by a marked decrease in hepatic granuloma formation. These findings imply that longitudinal ingestion of Pairogen attenuates *R. aurantiacus*-induced granulomatous inflammation by regulating the redox state in tissues and cells. Numerous studies have indicated that HO-1 possesses anti-inflammatory and anti-oxidative properties and that its induction is an adaptive defense mechanism to protect cells and tissues against injury in many diseases.[24,36] In our *in vitro* experiments, stimulation with heat-killed *R. aurantiacus* resulted in a higher level of HO-1 gene expression in the macrophages from F1 mice treated with 10-fold-diluted Pairogen compared with that in the cells from F1 mice received water, suggesting that the negative regulation of *R. aurantiacus*-induced inflammation by Pairogen is partially dependent on HO-1 production. Evidence suggests that the immune response is a redox-regulated process and that the redox state of resting immune cells determines the type and extent of immune response to pathogen stimulation.[37,38] The importance of redox homeostasis is further supported by the present study in which the coordination of the cellular redox state by Pairogen contributes to depression of excessive inflammatory and immune responses to *R. aurantiacus* infection in mice.

On the basis of these data, we conclude that longitudinal administration of Pairogen prior to infection augments their resistance to bacterial infection and suppresses excessive cytokine expression by modulating the cellular redox state in *R. aurantiacus*-infected mice, which consequently result in accelerated bacterial clearance, enhanced survival, and suppression of granulomatous inflammation. Moreover, the effects of Pairogen can be enhanced in mouse progeny that also ingest Pairogen, suggesting that the well-controlled redox state of immune cells by Pairogen in parental generation effectively affects the immunity and disease resistance of progeny. Our findings provide the basis for the application of Pairogen as a potential redox regulator in combating infectious disease and improving health.

Acknowledgments The authors thank Akatsuka Co., Mie, Japan for supply of Pairogen. This work was also supported by a generous grant from Akatsuka Co.

REFERENCES

1) Hirobe T. Ferrous ferric chloride induces the differentiation of cultured mouse epidermal melanocytes additionally with herbal medicines. *J. Health Sci.*, **55**, 86–94 (2009).
2) Hirobe T. Ferrous ferric chloride stimulates the proliferation of human skin keratinocytes, melanocytes, and fibroblasts in culture. *J. Health Sci.*, **55**, 447–455 (2009).
3) Sugi J, Yamashita S. The method for obtaining ferrous ferric chloride. *Bull. Soc. Sea Water Sci. Japan*, **42**, 11 (1991).
4) Hirobe T. Ferrous ferric chloride stimulates the proliferation and differentiation of cultured keratinocytes and melanocytes in the epidermis of neonatal mouse skin. *J. Health Sci.*, **53**, 576–584 (2007).
5) Hasegawa S, Meguro A, Shimizu M, Nishimura T, Kunoh H. The ceramic bead that is suitable for a carrier of plant-rooting accelerator, *Streptomyces* sp. MBR-52. *Actinomycetologica*, **20**, 23–29 (2006).
6) Hirobe T. Stimulation of the proliferation and differentiation of skin cells by ferrous ferric chloride from a distance. *Biol. Pharm. Bull.*, **34**, 987–995 (2011).
7) Hirobe T. Ferrous ferric chloride stimulates the skin cell function and hair growth in mice. *Biol. Pharm. Bull.*, **32**, 1347–1353 (2009).
8) Bergstrom KS, Sham HP, Zarepour M, Vallance BA. Innate host responses to enteric bacterial pathogens: a balancing act between resistance and tolerance. *Cell. Microbiol.*, **14**, 475–484 (2012).
9) Kawai T, Akira S. The role of pattern-recognition receptors in innate immunity: update on Toll-like receptors. *Nat. Immunol.*, **11**, 373–384 (2010).
10) Aitken SL, Corl CM, Sordillo LM. Immunopathology of mastitis: insights into disease recognition and resolution. *J. Mammary Gland Biol. Neoplasia*, **16**, 291–304 (2011).
11) Jarry A, Bossard C, Bou-Hanna C, Masson D, Espaze E, Denis MG, Laboisse CL. Mucosal IL-10 and TGF-β play crucial roles in preventing LPS-driven, IFN-γ-mediated epithelial damage in human colon explants. *J. Clin. Invest.*, **118**, 1132–1142 (2008).
12) Hoebe K, Janssen E, Beutler B. The interface between innate and adaptive immunity. *Nat. Immunol.*, **5**, 971–974 (2004).
13) van der Poll T, van Zoelen MA, Wiersinga WJ. Regulation of pro- and anti-inflammatory host responses. *Contrib. Microbiol.*, **17**, 125–136 (2011).
14) Fernandes AF, Zhou J, Zhang X, Bian Q, Sparrow J, Taylor A, Pereira P, Shang F. Oxidative inactivation of the proteasome in retinal pigment epithelial cells. A potential link between oxidative stress and up-regulation of interleukin-8. *J. Biol. Chem.*, **283**, 20745–20753 (2008).
15) Chen T, Lin X, Xu J, Tan R, Ji J, Shen P. Redox imbalance provokes deactivation of macrophages in sepsis. *Proteomics Clin. Appl.*, **3**, 1000–1009 (2009).
16) Haddad JJ. Redox regulation of pro-inflammatory cytokines and IκB-α/NF-κB nuclear translocation and activation. *Biochem. Biophys. Res. Commun.*, **296**, 847–856 (2002).
17) Victor VM, Rocha M, De la Fuente M. Immune cells: free radicals and antioxidants in sepsis. *Int. Immunopharmacol.*, **4**, 327–347 (2004).
18) Rahman I, MacNee W. Regulation of redox glutathione levels and gene transcription in lung inflammation: therapeutic approaches. *Free Radic. Biol. Med.*, **28**, 1405–1420 (2000).
19) Asano M, Minagawa T, Ohmichi M, Hiraga Y. Detection of endogenous cytokines in sera or in lymph nodes obtained from patients

with sarcoidosis. *Clin. Exp. Immunol.*, **84**, 92–96 (1991).
20) Yimin, Kohanawa M, Ozaki M, Haga S, Fujikawa K, Zhao S, Kuge Y, Tamaki N. Mutual modulation between interleukin-10 and interleukin-6 induced by *Rhodococcus aurantiacus* infection in mice. *Microbes Infect.*, **10**, 1450–1458 (2008).
21) Yimin, Kohanawa M. A regulatory effect of the balance between TNF-α and IL-6 in the granulomatous and inflammatory response to *Rhodococcus aurantiacus* infection in mice. *J. Immunol.*, **177**, 642–650 (2006).
22) Giacomini E, Iona E, Ferroni L, Miettinen M, Fattorini L, Orefici G, Julkunen I, Coccia EM. Infection of human macrophages and dendritic cells with *Mycobacterium tuberculosis* induces a differential cytokine gene expression that modulates T cell response. *J. Immunol.*, **166**, 7033–7041 (2001).
23) Yrlid U, Svensson M, Johansson C, Wick MJ. *Salmonella* infection of bone marrow-derived macrophages and dendritic cells: influence on antigen presentation and initiating an immune response. *FEMS Immunol. Med. Microbiol.*, **27**, 313–320 (2000).
24) Otterbein LE, Soares MP, Yamashita K, Bach FH. Heme oxygenase-1: unleashing the protective properties of heme. *Trends Immunol.*, **24**, 449–455 (2003).
25) Ha EM, Oh CT, Ryu JH, Bae YS, Kang SW, Jang IH, Brey PT, Lee WJ. An antioxidant system required for host protection against gut infection in *Drosophila*. *Dev. Cell*, **8**, 125–132 (2005).
26) Murapa P, Ward MR, Gandhapudi SK, Woodward JG, D'Orazio SE. Heat shock factor 1 protects mice from rapid death during *Listeria monocytogenes* infection by regulating expression of tumor necrosis factor alpha during fever. *Infect. Immun.*, **79**, 177–184 (2011).
27) Yimin, Kohanawa M, Minagawa T. Up-regulation of granulomatous inflammation in interleukin-6 knockout mice infected with *Rhodococcus aurantiacus*. *Immunology*, **110**, 501–506 (2003).
28) Lee IT, Yang CM. Role of NADPH oxidase/ROS in pro-inflammatory mediators-induced airway and pulmonary diseases. *Biochem. Pharmacol.*, **84**, 581–590 (2012).
29) Palacio JR, Markert UR, Martínez P. Anti-inflammatory properties of *N*-acetylcysteine on lipopolysaccharide-activated macrophages. *Inflamm. Res.*, **60**, 695–704 (2011).
30) Russo I, Luciani A, De Cicco P, Troncone E, Ciacci C. Butyrate attenuates lipopolysaccharide-induced inflammation in intestinal cells and Crohn's mucosa through modulation of antioxidant defense machinery. *PLoS ONE*, **7**, e32841 (2012).
31) Fernández V, Tapia G, Varela P, Romanque P, Cartier-Ugarte D, Videla LA. Thyroid hormone-induced oxidative stress in rodents and humans: a comparative view and relation to redox regulation of gene expression. *Comp. Biochem. Physiol. C Toxicol. Pharmacol.*, **142**, 231–239 (2006).
32) Song M, Kellum JA, Kaldas H, Fink MP. Evidence that glutathione depletion is a mechanism responsible for the anti-inflammatory effects of ethyl pyruvate in cultured lipopolysaccharide-stimulated RAW 264.7 cells. *J. Pharmacol. Exp. Ther.*, **308**, 307–316 (2004).
33) Victor VM, De la Fuente M. Immune cells redox state from mice with endotoxin-induced oxidative stress. Involvement of NF-κB. *Free Radic. Res.*, **37**, 19–27 (2003).
34) Wu SJ, Ng LT. Tetrandrine inhibits proinflammatory cytokines, iNOS and COX-2 expression in human monocytic cells. *Biol. Pharm. Bull.*, **30**, 59–62 (2007).
35) Hernández-Ledesma B, Hsieh CC, de Lumen BO. Antioxidant and anti-inflammatory properties of cancer preventive peptide lunasin in RAW 264.7 macrophages. *Biochem. Biophys. Res. Commun.*, **390**, 803–808 (2009).
36) Wu ML, Ho YC, Lin CY, Yet SF. Heme oxygenase-1 in inflammation and cardiovascular disease. *Am. J. Cardiovasc. Dis.*, **1**, 150–158 (2011).
37) Murata Y, Ohteki T, Koyasu S, Hamuro J. IFN-γ and pro-inflammatory cytokine production by antigen-presenting cells is dictated by intracellular thiol redox status regulated by oxygen tension. *Eur. J. Immunol.*, **32**, 2866–2873 (2002).
38) Rubartelli A, Gattorno M, Netea MG, Dinarello CA. Interplay between redox status and inflammasome activation. *Trends Immunol.*, **32**, 559–566 (2011).